Kinetics of Channel Formation in Bilayer Lipid Membranes (BLMs) and Tethered BLMs: Monazomycin and Melittin

ARTICLE *in* LANGMUIR · JUNE 2007

Impact Factor: 4.46 · DOI: 10.1021/la0636560 · Source: PubMed

2 AUTHORS:

Lucia Becucci
University of Florence
72 PUBLICATIONS **1,376** CITATIONS
SEE PROFILE

Rolando Guidelli
University of Florence
226 PUBLICATIONS **3,889** CITATIONS
SEE PROFILE

Kinetics of Channel Formation in Bilayer Lipid Membranes (BLMs) and Tethered BLMs: Monazomycin and Melittin

Lucia Becucci and Rolando Guidelli*

Department of Chemistry, Florence University, Sesto Fiorentino (Firenze), Italy

Received December 18, 2006. In Final Form: February 27, 2007

The kinetics of channel formation by the polyene-like antibiotic monazomycin, both in a bilayer lipid membrane (BLM) and in a tethered BLM (tBLM), and by the peptide melittin in a tBLM, is investigated. Stepping the applied potential from a value at which channels are not formed to one at which they are formed yields current vs time curves that are sigmoidal on a BLM, while they show a maximum on a tBLM; in the latter case, sigmoidal curves are obtained by plotting the charge against time. These curves are interpreted on the basis of a general kinetic model, which accounts for the potential-dependent penetration of adsorbed monomeric molecules into the lipid bilayer, followed by their aggregation with channel formation by a mechanism of nucleation and growth. In the case of monazomycin, which is present in the solution in the form of relatively hydrophilic clusters and is adsorbed as such on top of the lipid bilayer, penetration into the bilayer following a potential jump is assumed to be preceded by a potential-independent disaggregation of the adsorbed clusters into adsorbed monomers.

Introduction

It is well-known that many channel-forming peptides, such as alamethicin and melittin, when added to the solution bathing one side of a bilayer lipid membrane (BLM), are adsorbed flat on this side of the BLM, provided that the transmembrane potential is close to zero. If the transmembrane potential on the opposite side of the membrane is then decreased to a sufficiently negative value, the peptide monomers penetrate the lipid bilayer and form channels. These are regarded as bundles of membrane-spanning α-helical molecules surrounding a central pore.[1] One face of the helices is hydrophobic, while the other is hydrophilic, due to the presence of carbonyl groups. The hydrophobic faces are directed outward, so as to establish favorable interactions with the hydrocarbon tails of the lipid bilayer. The hydrophilic faces are directed inward, making the polar residues available for favorable interactions with permeant ions and/or water molecules. A similar model is also assumed for channel-forming proteins, such as potassium channels, whose molecular weights are 2 orders of magnitude greater than that of channel-forming peptides. Due to their much simpler structure, channel-forming peptides are often viewed as models of channel-forming proteins.

The formation of bundles is expected to proceed via a mechanism of nucleation and growth. If this mechanism controls the kinetics of the whole process of channel formation, it has been shown that potential jumps from a value at which bundles are not yet formed to one were they are formed yield sigmoidal potentiostatic current vs time curves, referred to as "voltage−clamp" curves.[2] Several channel-forming antibiotics, peptides, and proteins exhibit sigmoidal voltage−clamp curves. A typical example is provided by the polyene-like antibiotic monazomycin, whose sigmoidal voltage−clamp curves[3,4] were interpreted on the basis of a standard chemical kinetics formulation, under the assumption that monazomycin entry into and exit from the membrane is autocatalytic.[5,6] Sigmoidal voltage−clamp curves were also reported for BLMs incorporating melittin.[7] Alamethicin-doped membranes do not show sigmoidal voltage−clamp curves under normal experimental conditions;[8] it is possible that a mechanism of nucleation and growth is obscured by a preceding, rate-determining penetration of alamethicin monomers into the BLM. However, membranes incorporating alamethicin do yield sigmoidal voltage−clamp curves at a pressure of 100 MPa.[9] These were also observed at atmospheric pressure,[8] but only over times very short compared to those required to develop the full response to a voltage step. At high pressures, the sigmoidal shape was interpreted by a three-state model in which a nonconducting surface state is followed by a nonconducting precursor state, and then by a conducting state.[10] Among the channel-forming proteins yielding sigmoidal voltage−clamp curves, by far the most familiar are undoubtedly the potassium channels of the squid giant axon investigated by Hodgkin and Huxley,[11] who developed an empirical kinetic description of these curves. Further proteins yielding sigmoidal voltage−clamp curves are the voltage-gated proton channels.[12−14]

Lipid bilayers tethered to a metal surface via a hydrophilic "spacer", often called tethered bilayer lipid membranes (tBLMs), provide a friendly environment to channel-forming peptides and proteins, thus maintaining their functionally active state and allowing an investigation of their function. The interposition of a hydrophilic layer between the metal surface and the lipid bilayer is particularly important to create the hydrophilic environment needed for the proper folding of the extramembrane section of integral proteins and to allow an ionic flow across the lipid bilayer, upon incorporation of an ion channel.[15] tBLMs are obtained by

* rolando.guidelli@unifi.it.

(1) Sansom, M. S. P. *Prog. Biophys. Mol. Biol.* **1991**, *55*, 139−235.
(2) Becucci, L.; Moncelli, M. R.; Guidelli, R. *J. Am. Chem. Soc.* **2003**, *125*, 3785−3792.
(3) Muller, R. U.; Finkelstein, A. *J. Gen. Physiol.* **1972**, *60*, 263−284.
(4) Muller, R. U.; Finkelstein, A. *J. Gen. Physiol.* **1972**, *60*, 285−306.
(5) Muller, R. U.; Orin, G.; Peskin, C. S. *J. Gen. Physiol.* **1981**, *78*, 171−200.
(6) Muller, R. U.; Peskin, C. S. *J. Gen. Physiol.* **1981**, *78*, 201−229.
(7) Tosteson, M. T.; Alvarez, O.; Hubbell, W.; Bieganski, R. M.; Attenbach, C.; Caporales, L. H.; Levy, J. J.; Nutt, R. F.; Rosenblatt, M.; Tosteson, D. C. *Biophys. J.* **1990**, *58*, 1367−1375.
(8) Mauro, A.; Nanavati, R. P.; Heyer, E. *Proc. Natl. Acad. Sci. U.S.A.* **1972**, *69*, 3742−3744.
(9) Bruner, L. J.; Hall, J. E. *Biophys. J.* **1983**, *44*, 39−47.
(10) Bruner, L. J. *J. Theor. Biol.* **1985**, *117*, 265−276.
(11) Hodgkin, A. L.; Huxley, A. F. *J. Physiol.* **1952**, *117*, 500−544.
(12) DeCoursey, T. E.; Cherny, V. V. *Biophys. J.* **1996**, *71*, 182−193.
(13) Cherny, V. V.; Markin, V. S.; DeCoursey, T. E. *J. Gen. Physiol.* **1995**, *105*, 861−896.
(14) Cherny, V. V.; DeCoursey, T. E. *J. Gen. Physiol.* **1999**, *114*, 819−838.
(15) Guidelli, R.; Aloisi, G.; Becucci, L.; Dolfi, A.; Moncelli, M. R.; Tadini Buoninsegni, F. *J. Electroanal. Chem.* **2001**, *504*, 1−28.

10.1021/la0636560 CCC: $37.00
Published on Web 04/10/2007

first self-assembling on a gold[16−21] or mercury electrode[22−25] a monolayer of a thiolipid, which consists of a hydrophilic spacer terminated at one end with a sulfhydryl or disulfide group for anchoring to the metal surface and covalently linked at the other end to the polar head of a phospholipid. A lipid monolayer is then self-assembled on top of the thiolipid monolayer, by exploiting the hydrophobic interactions that bring the alkyl chains of the two monolayers into contact with each other, with the polar heads of the lipid turned toward the aqueous solution.

In recent work carried out in the present laboratory, use has been made of a mercury-supported tBLM prepared with a particularly convenient thiolipid used by Naumann[19−21] for the preparation and characterization of tBLMs on gold. This thiolipid, named DPTL, consists of a tetraethyleneoxy chain covalently linked to a lipoic acid residue for anchoring to the metal at one end, and bound via ether linkages to two phytanyl chains at the other end. The tBLM is obtained by anchoring a DPTL monolayer to a mercury electrode and by self-assembling a diphytanoylphosphatidylcholine monolayer on top of it. This gives rise to a lipid bilayer separated from the mercury surface by the tetraethyleneoxy chain, which acts as a hydrophilic ionic reservoir on the metal side of the lipid bilayer. Thanks to its liquid nature, mercury provides a defect-free surface to the self-assembling film, and imparts a high fluidity to the tBLM by allowing the lateral movement of the thiolipid molecules anchored to its surface.

This work describes an investigation of the kinetics of channel formation by the antibiotic monazomycin in both a BLM and a tBLM, and by the peptide melittin in a tBLM. Both melittin and monazomycin form channels in biological membranes, by aggregation of monomeric units. Melittin is the major component of the venom of the honey bee. It is a polypeptide that comprises 26 amino acid residues, including 5 with positively charged side chains in addition to the NH_2-terminal glycine. Four of these charges are in the highly basic C-terminal tetrapeptide sequence Lys-Arg-Lys-Arg, with only the N-terminal amino group and Lys-7 in the N-terminal sequence.[7] Due to the high dipole moment of melittin, when a negative voltage is applied on the side of the membrane opposite to that where this peptide has been added, its NH_2-terminal end is pushed through the membrane, causing melittin to span the lipid bilayer. Monazomycin is an antibiotic produced by streptomyces; its molecular weight is about 1200, and its structure, reported in the chem-faculty.ucsd.edu/kobayashi/research.html web site, is related to that of polyene antibiotics. Monazomycin has an amino group that gives a positive charge to the molecule at neutral pH. When monazomycin is added in micromolar amounts to one side of a bilayer, membrane conductance becomes strongly voltage-dependent.

By stepping the applied potential from a value at which melittin and monazomycin channels are not formed to one at which they are formed, the resulting current vs time curves are sigmoidal on a BLM, while they show a maximum on a tBLM; in the latter case, sigmoidal curves are obtained by plotting the potentiostatic charge against time. These curves are interpreted on the basis of a general kinetic model, which accounts for the potential-dependent penetration of adsorbed monomeric molecules into the lipid bilayer, followed by their aggregation with channel formation by a mechanism of nucleation and growth. In the case of monazomycin, which is present in the solution in the form of relatively hydrophilic clusters and is adsorbed as such on top of a lipid bilayer, penetration into the bilayer following a potential jump is assumed to be preceded by a potential-independent disaggregation of the adsorbed clusters into adsorbed monomers by a mechanism of nucleation and growth of holes into the cluster.

Experimental Section

The water used was obtained from water produced by an inverted osmosis unit, upon distilling it once and then distilling the water so obtained from alkaline permanganate. Merck suprapure KCl was baked at 500 °C before use to remove any organic impurities. Diphytanoylphosphatidylcholine (PC) was purchased in chloroform solution from Avanti Polar Lipids (Birmingham, AL). The 2,3-di-*O*-phytanyl-*sn*-glycerol-1-tetraethylene-glycol-D,L-α lipoic acid ester lipid (DPTL) was a generous gift from Dr. Renate Naumann and Prof. Wolfgang Knoll (Max Plank Institute for Polymer Research in Mainz). Melittin was purchased from Sigma. The monazomycin was a generous gift by Prof. Joel Coen. PC solutions were prepared by diluting proper amounts of stock solutions of this phospholipid with pentane. Solutions of 0.2 mg/mL DPTL in ethanol were prepared from a 2 mg/mL solution of DPTL in ethanol. Stock solutions of this thiolipid were stored at −18 °C. Stock solutions of 7×10^{-5} M melittin in water and of 0.01 M monazomycin in methanol were stored at +4 °C.

All measurements were carried out in aqueous 0.1 M KCl. Use was made of a homemade hanging mercury drop electrode (HMDE), described elsewhere.[26] A homemade glass capillary with a finely tapered tip, about 1 mm in outer diameter, was employed. Capillary and mercury reservoir were thermostated at 25 ± 0.1 °C in a water-jacketed box to avoid any changes in drop area due to a change in temperature. One glass electrolysis cell containing the aqueous solution and a small glass vessel containing the ethanol solution of the thiolipid were placed on a movable support inside the box.[27] The HMDE and the support were moved vertically and horizontally, respectively, by means of two oleodynamic systems that ensured the complete absence of vibrations. Chronocoulometric measurements were carried out with an Autolab instrument (Echo Chemie) supplied with an FRA2 module for impedance measurements, SCAN-GEN scan generator, and GPES 4.9005 Beta software. Potentials were measured vs an Ag|AgCl electrode immersed in the 0.1 M KCl working solution and are referenced to this electrode.

Monolayers of DPTL were self-assembled on the HMDE by keeping the mercury drop immersed in the small vessel containing the thiolipid solution for about 20 min. In the meantime, a lipid solution in pentane was spread on the surface of the aqueous solution in the glass cell, in an amount corresponding to five to six lipid monolayers, and the pentane was allowed to evaporate. Using the oleodynamic system, the DPTL-coated HMDE was then extracted from the vessel, washed with ethanol to remove the excess of adsorbed thiolipid, and kept in a N_2 atmosphere for the time strictly necessary to allow the solvent to evaporate. Immediately afterward, the electrolysis cell containing the aqueous solution on whose surface

(16) Cornell, B. A.; Braach-Maksvytis, V. L. B.; King, L. G.; Osman, P. D. J.; Raguse, B.; Wieczorek, L.; Pace, R. J. *Nature (London)* **1997**, *387*, 580−583.
(17) Naumann, R.; Jonczyk, A.; Kopp, R.; van Esch, J.; Ringsdorf, H.; Knoll, W.; Gräber, P. *Angew. Chem., Int. Ed. Engl.* **1995**, *34*, 2056−2058.
(18) Naumann, R.; Schmidt, E. K.; Jonczyk, A.; Fendler, K.; Kadenbach, B.; Liebermann, T.; Offenhäusser, A.; Knoll, W. *Biosens. Bioelectron.* **1999**, *14*, 651−662.
(19) Naumann, R.; Schiller, S. M.; Giess, F.; Grohe, B.; Hartman, K. B.; Kärcher, I.; Köper, I.; Lübben, J.; Vasilev, K.; Knoll, W. *Langmuir* **2003**, *19*, 5435−5443.
(20) Naumann, R.; Walz, D.; Schiller, S. M.; Knoll, W. *J. Electroanal. Chem.* **2003**, *550*−*551*, 241−247.
(21) Schiller, S. M.; Naumann, R.; Lovejoy, K.; Kunz, H.; Knoll, W. *Angew. Chem., Int. Ed.* **2003**, *42*, 208−211.
(22) Becucci, L.; Moncelli, M. R.; Guidelli, R. *Langmuir* **2003**, *19*, 3386−3392.
(23) Becucci, L.; Moncelli, M. R.; Naumann, R.; Guidelli, R. *J. Am. Chem. Soc.* **2005**, *127*, 13316−13323.
(24) Becucci, L.; Moncelli, M. R.; Guidelli, R. *Langmuir* **2006**, *22*, 1341−1346.
(25) Becucci, L.; Romero Léon, R.; Moncelli, M. R.; Rovero, P.; Guidelli, R. *Langmuir* **2006**, *22*, 6644−6650.
(26) Moncelli, M. R.; Becucci, L. *J. Electroanal. Chem.* **1997**, *433*, 91−96.
(27) Tadini Buoninsegni, F.; Herrero, R.; Moncelli, M. R. *J. Electroanal. Chem.* **1998**, *452*, 33−42.

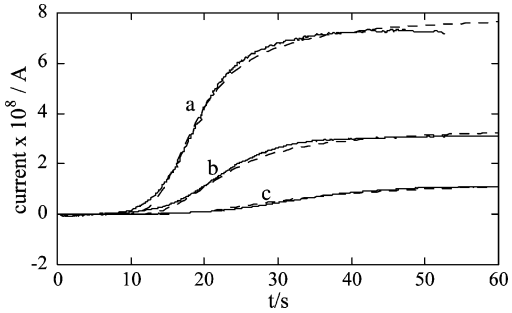

Figure 1. The solid curves are three successive current vs time curves on the same BLM following transmembrane potential jumps from $E = 0$ to $E = -60$ mV (a), -55 mV (b), and -50 mV (c), in aqueous 0.1 M KCl containing 6.25×10^{-7} M monazomycin (5). The corresponding dashed curves were calculated as described in the text using the parameters $\theta_0 = 0.1$, $n = 2$, and $k_{h,N}\upsilon_{h,R}^2 = 0.016$ s^{-3} for all three curves; p and $k_N k_R^2$ were given the following values: (a) 1 and 15 s^{-3}; (b) 0.438 and 130 s^{-3}; (c) 0.163 and 1250 s^{-3}. The three calculated currents were matched to the experimental ones by multiplying them by the same factor, 80.

the lipid film had been previously spread was brought below the HMDE, and the latter was lowered so as to immerse it into the aqueous solution across the lipid film; this procedure causes a lipid monolayer to self-assemble on top of the DPTL monolayer, giving rise to a lipid bilayer interposed between the hydrophilic moiety of the thiolipid and the aqueous solution. The applied potential was then repeatedly scanned over a potential range from -0.200 to -1.200 V while continuously monitoring the curve of the quadrature component, Y'', of the electrode admittance at 75 Hz against the applied potential, E, using ac voltammetry, until a stable Y'' vs E curve was attained. The minimum differential capacity of the resulting (DPTL/lipid)-coated mercury ranged from 0.55 to 0.65 μF cm^{-2}, and was therefore close to the capacity, $\sim$0.8 μF cm^{-2}, of a solvent-free black lipid membrane. Melittin and monazomycin were incorporated in this tBLM by simply adding their stock solutions to the electrolysis cell in an amount corresponding to 1.4×10^{-7} M and 2.5×10^{-7} M, respectively. The solution was, then, stirred for 5 min, while keeping the electrode at an applied potential of -0.500 V.

Results

The solid voltage−clamp curves in Figure 1 were obtained in phosphatidylethanolamine BLMs symmetrically bathed by unbuffered 0.1 M KCl, with the cis side of the membrane containing 6.25×10^{-7} M monazomycin. They were obtained by stepping the transmembrane potential on the trans side from 0 to -60 mV (a), -55 mV (b), and -50 mV (c). The potential was held at $+100$ mV for 1 min and then set at 0 mV for 15 s before each step. The curves were extracted from Figure 5 of Muller et al.[5] The corresponding dashed curves were obtained on the basis of the kinetic model to be described in the following. The voltage−clamp curves are sigmoidal in shape with a long foot, and the height of their plateau decreases as the transmembrane potential is stepped from zero to progressively lower negative values.

When analogous potential jumps are carried out with a tBLM incorporating monazomycin, the resulting current vs time curves, once corrected for the background current, attain a maximum and then decay to zero. This difference in behavior is due to the fact that the translocating ions cannot diffuse freely on the trans side of the lipid bilayer, as in the case of a BLM. Rather, they accumulate into the hydrophilic spacer moiety of the tBLM until they saturate it. Sigmoidal curves are obtained if the charge, rather than the current, is recorded against time. Figure 2 shows the change vs time curves obtained by stepping the applied potential from -0.200 V to more negative potentials on a tBLM

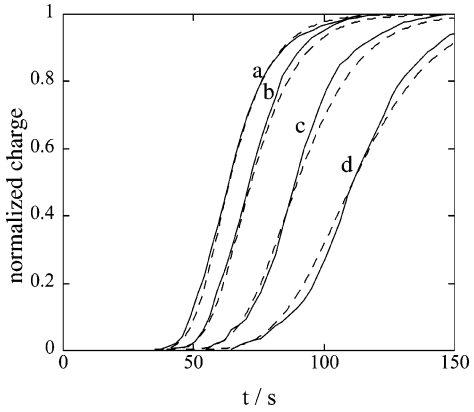

Figure 2. The solid curves are four successive charge vs time curves on a tBLM following potential jumps from the same initial value of -0.200 V to the final values -0.850 V (a), -0.825 V (b), -0.800 V (c), and -0.775 V (d), in aqueous 0.1 M KCl containing 2.5×10^{-7} M monazomycin. The height of the plateau of the curves is normalized to unity. The corresponding dashed curves were calculated as described in the text using the parameters $\theta_0 = 0.1$, $n = 2$, $k_{h,N}\upsilon_{h,R}^2 = 5 \times 10^{-4}$ s^{-3}, and $k_{d,R} = 7 \times 10^{-3}$ cm^2 s^{-1} for all four curves; p and $k_N k_R^2$ were given the following values: (a) 1 and 15 s^{-3}; (b) 0.4 and 130 s^{-3}; (c) 0.06 and 4×10^3 s^{-3}; (d) 0.09 and 5×10^3 s^{-3}.

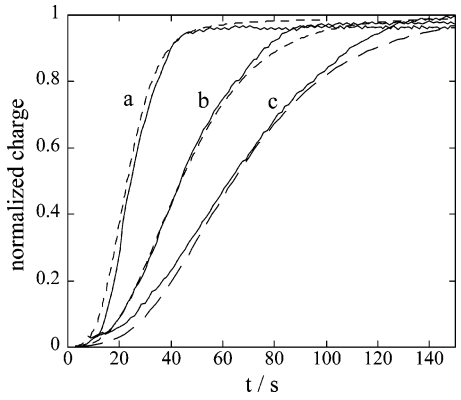

Figure 3. The solid curves are three successive charge vs time curves on a tBLM following potential jumps from the same initial value of -0.200 V to the final values -1.050 V (a), -1.000 V (b), and -0.950 V (c) in aqueous 0.1 M KCl containing 1.4×10^{-7} M melittin. The height of the plateau of the curves is normalized to unity. The corresponding dashed curves were calculated as described in the text using the parameters $\theta_0 = 0.2$, $n = 2$, and $k_N k_R^2 = 0.05$ s^{-3} for all three curves; p and $k_{d,R}$ were given the following values: (a) 1 and 0.02 cm^2 s^{-1}; (b) 0.8 and 5×10^{-3} cm^2 s^{-1}; (c) 0.6 and 3.5×10^{-3} cm^2 s^{-1}.

incorporating monazomycin from its 2.5×10^{-7} M solution in aqueous 0.1 M KCl.

The maximum limiting value attained by the charge in all these curves is practically the same. In fact, this limiting value is just a measure of the maximum amount of potassium ions that can be accommodated into the hydrophilic spacer. The curves in Figure 2 are normalized to unity for convenience, in order to compare them with the corresponding calculated curves. These curves are characterized by a long induction period (the long foot), analogous to that exhibited by the current vs time curves on a BLM.

A sigmoidal shape is also exhibited by charge vs time curves following potential jumps on a tBLM incorporating melittin from its 1.4×10^{-7} M solution in aqueous 0.1 M KCl (see Figure 3). However, distinct from the curves of monazomycin, they exhibit

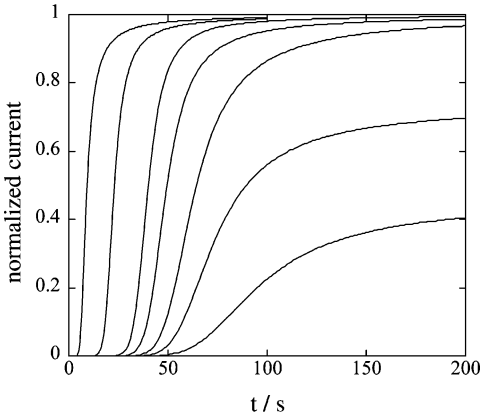

Figure 4. Current vs time curves calculated by accounting for initial disaggregation of horizontal clusters by using the parameters $\theta_0 = 0.1$ and $n = 2$ for all curves. The parameters $2\pi k_{h,N}\upsilon_{h,R}^2$, $k_N k_R^2$, and p were given the following values: (a) 1 s^{-3}, 100 s^{-3}, 1; (b) 0.01 s^{-3}, 100 s^{-3}, 1; (c) 0.001 s^{-3}, 100 s^{-3}, 1; (d) 0.001 s^{-3}, 10 s^{-3}, 1; (e) 0.001 s^{-3}, 1 s^{-3}, 1; (f) 0.001 s^{-3}, 1 s^{-3}, 0.75; (g) 0.001 s^{-3}, 1 s^{-3}, 0.5. The maximum current was normalized to unity by multiplying all currents by the factor 2.3×10^{-4}.

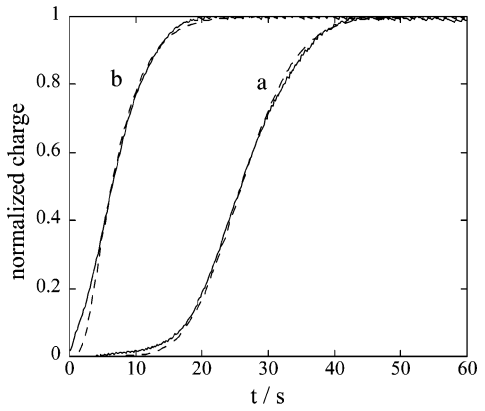

Figure 5. The solid curves are charge vs time curves on a tBLM following potential jumps from −0.200 V to −1.050 V in aqueous 0.1 M KCl containing 1.4×10^{-7} M melittin. Curve (a) was obtained after keeping the potential at −0.200 V for 15 min; curve (b) was obtained after keeping the potential at −1.050 V for 150 s, stepping it back to −0.200 V and recording the subsequent potential jump to −1.050 V immediately afterwards. The dashed curve (a) was calculated using the parameters $\theta_0 = 0.2$, $n = 2$, $k_{h,N}\upsilon_{h,R}^2 = 0.08$ s^{-3}, $k_N k_R^2 = 0.05$ s^{-3}, $k_{d,R} = 0.04$ cm^2 s^{-1}, and $p = 1$; the dashed curve (b) was calculated using the parameters $\theta_0 = 0.2$, $n = 2$, $k_N k_R^2 = 40$ s^{-3}, $k_{d,R} = 0.02$ cm^2 s^{-1}, and $p = 1$.

a short induction period and a slope that decreases notably with a decrease in the negative final potential.

Discussion

The Model of Nucleation and Growth. The process of disruption of clusters adsorbed on top of a BLM (henceforth referred to as "horizontal clusters"), the penetration of the resulting "horizontal monomers" into the lipid bilayer following a suitable transmembrane-potential jump, and the aggregation of the monomers incorporated in the BLM (henceforth referred to as the "vertical monomers") into channel-forming "vertical clusters" will be treated as consecutive, strictly correlated, events.

The kinetic process of disruption of horizontal clusters will be treated as a nucleation and growth of holes within the surface area covered by them on top of the BLM. By "nucleation" of holes, we mean the quasi-reversible detachment of an initial number of horizontal monomers from a horizontal cluster and their random intercalation with the water molecules. In other words, a hole is just a monomer that, upon detachment from a cluster, leaves behind a hole in the cluster. These horizontal monomers are considered to be detached and reaggregate to horizontal clusters in a quasi-reversible manner, until the size of the holes in a cluster attains a critical size beyond which the cluster undergoes an irreversible disruption. By "growth" of holes, we just mean this irreversible detachment of the residual monomers from the cluster, leading to its complete disruption.

Let θ_0 denote the fraction of the whole surface of the BLM initially covered by horizontal clusters. The disruption of the horizontal clusters starts at the instant at which the transmembrane potential on the opposite side of the BLM is stepped to a sufficiently negative value: this instant is taken as the origin of the time axis. Let S_h denote the time-dependent ratio of the area covered by holes (i.e., the horizontal monomers being released from the horizontal clusters) to that, θ_0, initially covered by horizontal clusters. Since the nucleation of holes takes place within the surface area covered by clusters, the nucleation rate $\upsilon_{h,N}$ will be set proportional to this fractional surface area, $\theta_0(1 - S_h)$, according to a proportionality constant $k_{h,N}$. Upon ascribing, for simplicity, a circular shape to the growing holes, the rate $\upsilon_{h,R}$ of their radial growth will be regarded as roughly independent of the surface coverage, $\theta_0(1 - S_h)$, by clusters. This assumption is particularly justified during the initial growth of holes in a cluster, when the holes are almost completely surrounded by the horizontal monomeric units forming the given cluster. Such an assumption becomes rougher at later stages of cluster disruption, when, however, this assumption has a minor effect on the rate of the whole process. In fact, as the horizontal monomers are gradually formed, they are assumed to penetrate into the lipid bilayer with a probability p that is potential-dependent and increases as the transmembrane potential is stepped to progressively more negative values. The rate constant of nucleation of holes, $k_{h,N}$, and the rate of their radial growth, $\upsilon_{h,R}$, are assumed to be intrinsically independent of potential, since they involve horizontal molecules, whose dipole moments are practically normal to the electric field. However, they depend indirectly upon potential via the penetration probability p of the horizontal monomers. The ratio, S_h, of the area covered by horizontal monomers to that of horizontal clusters is estimated by first ignoring the overlapping of the growing holes and by then correcting for this neglect by using Avrami's approach[28−30] (see a detailed description of the nucleation-and-growth model outlined in the Supporting Information). In the expression of S_h, the rates of nucleation and growth are only present in the form of the $k_{h,N}\upsilon_{h,R}^2$ product. Therefore, only the single free parameter $\upsilon_{h,N}\upsilon_{h,R}^2$ is required to account for the kinetics of nucleation and growth of holes.

As the vertical monomers are formed, they start to nucleate, giving rise to channel-forming vertical clusters. Denoting by S the ratio of the area covered by vertical clusters to that covered by both vertical monomers and vertical clusters, the fraction of the whole electrode surface covered by vertical monomers is given by $\Theta = S_h\theta_0 p(1 - S)$. Clusters of vertical monomers resulting from a series of consecutive collisions are characterized by a critical size (the nucleus), below which they have a higher tendency to shrink by releasing one unit than to grow by aggregation of a further unit, and above which they have a practically irreversible tendency to increase. As in the case of nucleation and growth of holes, the formation of this critical size from monomeric units is referred to as nucleation, and the

(28) Avrami, M. *J. Chem. Phys.* **1939**, *7*, 1103−1112.
(29) Avrami, M. *J. Chem. Phys.* **1940**, *8*, 212−224.
(30) Avrami, M. *J. Phys. Chem.* **1941**, *9*, 177−184.

irreversible increase beyond the critical size as growth. If we denote by n the number of vertical monomers composing a nucleus, the elementary step yielding the nucleus consists of the incorporation of a monomer into an $(n - 1)$-meric subcritical cluster. This results from $(n - 1)$ elementary steps consisting of the incorporation of each monomeric unit into the immediately preceding subcritical cluster, starting from an initial monomer acting as a "nucleation center". If we assume that all steps preceding the step yielding the nucleus are in quasi-equilibrium, then the nucleation rate υ_N will be proportional to the nth power of the fractional surface coverage, $\Theta = S_h\theta_0 p(1 - S)$, by the vertical monomers randomly distributed in the monolayer, according to a nucleation rate constant k_N

$$dN/dt \equiv \upsilon_N = k_N\Theta^n \quad (1)$$

Here, N is the number of nuclei per unit surface area. Assuming for simplicity that the cross-sectional area A of a growing supercritical cluster is a circle of radius R, the rate of growth of A is given by the time derivative of πR^2. Moreover, it is proportional to the frequency of the successful impacts of the vertical monomers, of surface coverage Θ, with the circumference $2\pi R$ of the cluster, according to a proportionality constant k_R

$$dA/dt = d(\pi R^2)/dt = 2\pi R\, dR/dt = k_R 2\pi R\Theta \rightarrow dR/dt \equiv \upsilon_R = k_R\Theta \quad (2)$$

It follows that the rate υ_R of radial growth of a supercritical cluster is proportional to Θ according to the rate constant k_R. It should be stressed that the frequency of the successful impacts is not necessarily controlled by the two-dimensional diffusion of the vertical monomers within the lipid bilayer, but rather by the occurrence of a favorable mutual orientation of the cluster and of the aggregating vertical monomer. In analogy with the S_h ratio, the expression for the S ratio contains the $k_N k_R^2$ product as the only free parameter. Here too, S is calculated by first ignoring the possible overlapping of the growing vertical clusters and by then correcting for this neglect by using Avrami's approach.[28−30]

Finally, the current density I across the BLM induced by the transmembrane-potential jump is set proportional to the fractional surface coverage of the channel-forming vertical clusters, $S_h\theta_0 pS$, since each newly formed channel makes a contribution to this current. It should be noted that the fractional area $S_h\theta_0 pS$ should by no means be regarded as homogeneous. Rather, it should be regarded as consisting of separate channel-forming clusters of possibly different sizes dispersed in the BLM. The limiting value attained by I will clearly be given by $\theta_0 p$, since both S_h and S will ultimately tend to unity. The present model of nucleation and growth is entirely general. Thus, it only assumes that the elementary steps preceding the step yielding the nucleus are in quasi-equilibrium, and that the cluster growth beyond the nucleus proceeds irreversibly by activated aggregation of monomers to the growing cluster.

Figure 4 shows a series of current vs time curves calculated from the model, for different values of the overall rate $k_{h,N}v_{h,R}^2$ of nucleation and growth of holes in the horizontal clusters (namely, their rate of disaggregation) and of the overall rate $k_N k_{,R}^2$ of nucleation and growth of vertical clusters (namely, their rate of aggregation) with channel formation. In practice, if the rate of disaggregation of horizontal clusters decreases, while the rate of aggregation of vertical clusters remains constant, the long foot of the sigmoidal curve, which depends on the disaggregation rate, increases, while the slope of the rising section, which depends on the aggregation rate, remains substantially unchanged. On the other hand, if the disaggregation rate is kept constant while the aggregation rate decreases, the foot of the sigmoidal curve remains substantially unaltered, while the slope of the rising section decreases. Finally, if both the disaggregation and the aggregation rates are kept constant while the potential-dependent penetration probability p decreases with respect to its maximum unit value, the height of the plateau of the curve decreases, and this is accompanied by a slight decrease in the slope of the rising section.

Monazomycin in a BLM. Monazomycin, an antibiotic with a hydrophilic polyene-like structure, has been extensively investigated in past times. Sigmoidal current vs time curves on BLMs by the voltage−clamp technique were first reported by Muller and Finkelstein,[3] who also determined diffuse-layer effects of surface charge upon these curves.[4] The same authors, with Heyer,[31] proposed a model for the monazomycin channel consisting of approximately five molecules, each spanning the membrane with its NH_3^+ group on the trans side and with an uncharged group anchored to the cis side. The channel, lined by hydroxyl groups, should arise from the penetration of molecules lying parallel to the cis surface of the membrane, under the influence of a transmembrane potential negative on the trans side, followed by a potential independent aggregation of these molecules. The inactivation of the monazomycin-induced conductance at exceedingly negative transmembrane potentials was explained by monazomycin molecules crossing the membrane to the opposite (trans) side from which they were added.[32] An inactivation produced by addition of long-chain quaternary ammonium salts to the cis side was explained by these cations passing to the trans side through the monazomycin channels.[31]

Muller et al.[5] showed that the monazomycin-induced current vs time curves and their dependence upon the transmembrane potential E can be satisfactorily expressed by the following differential equation:

$$dg/dt = Ag[1 - (g/g_\infty)^B] \quad (3)$$

Here, $g = I/E$ is the conductance, g_∞ is its steady-state value, A is a rate constant, and B is an empirical constant equal to 0.7. A and g depend exponentially upon E and are proportional to a power of the monazomycin concentration, with a potential-independent exponent greater than unity. The initial exponential increase in conductance and the power dependence upon the monazomycin concentration lead Muller and Peskin[6] to postulate an autocatalytic step in the pathway of channel formation. Since this step is "formally" voltage-dependent, they derived eq 3 from a model, according to which a cluster M_α, of molecularity α, is present in solution or is directly adsorbed on top of the membrane in a "horizontal" orientation. M_α interacts, according to a potential-dependent kinetics, with a "vertical" cluster M_β, of molecularity β, incorporated in the membrane, yielding $(\alpha + \beta)/\beta$ M_β clusters. It is evident that this step will drag M_α clusters into the membrane more rapidly, the higher the concentration of the progressively formed M_β clusters, through an autocatalytic cycle. The membrane-spanning M_β clusters, which are assumed to be nonconducting, are then considered to associate into conducting clusters M_γ in a following step in quasi-equilibrium. The current across the membrane is considered to be proportional to the number of M_γ clusters. The formal inconsistency of the above autocatalytic step, according to which no current may ever flow in the absence of M_β clusters, was later removed by Muller and

(31) Heyer, E. J.; Muller, R. U.; Finkelstein, A. *J. Gen. Physiol.* **1976**, *67*, 703−729.
(32) Heyer, E. J.; Muller, R. U.; Finkelstein, A. *J. Gen. Physiol.* **1976**, *67*, 731−748.

Andersen[33] by postulating a potential-dependent penetration of horizontal clusters into the membrane running in parallel with the autocatalytic step, albeit at a much lower rate. In order to better account for the long initial "induction" period, these authors also postulated an oligomerization equilibrium in solution prior to the rate-determining autocatalytic step.

As a matter of fact, the mechanism by Muller and Peskin[6] contrasts somewhat with their initial considerations, according to which the amphipathic nature of monazomycin is expected to give rise to clusters with a hydrophobic core and a hydrophilic exterior in aqueous solution. Conversely, the clusters incorporated in the membrane should have a hydrophilic core and a hydrophobic exterior. Therefore, the passage from horizontal to vertical clusters should reasonably require an intermediate step involving a disaggregation of horizontal clusters into horizontal monomers, as assumed in the present model. At this stage of the process, the formation of horizontal clusters with a hydrophobic exterior from the horizontal monomers, prior to their subsequent incorporation, is highly improbable, since it would be opposed by unfavorable interactions with the water molecules surrounding a large portion of the adsorbed monomers. Therefore, horizontal monomers are the most probable candidates for a potential-dependent penetration into the membrane. Moreover, the potential-independent aggregation of vertical monomers into vertical clusters is per se an autocatalytic process, if it is controlled by nucleation-and-growth kinetics. Its "apparent" potential dependence is just due to the preceding penetration of horizontal monomers into the membrane, provided this is in quasi-equilibrium. Naturally, if the penetration step becomes rate-determining, current vs time curves are not expected to exhibit a sigmoidal shape, namely, a shape pointing to an autocatalytic step. Rather, they will tend to their steady-state value by constantly maintaining the concavity of the curve turned toward the time axis, as shown by the current vs time curves of alamethicin[8] at an ambient pressure. Sigmoidal current vs time curves of alamethicin have been reported at an elevated pressure of 100 MPa.[9] The various effects of pressure on alamethicin conductance indicate that high pressure slows down diffusion within the lipid bilayer but not within the aqueous phase. A slow diffusion of alamethicin monomers within the BLM may cause the nucleation-and-growth process to become the rate-limiting one, thus explaining the sigmoidal shape observed at high pressures.

The dashed curves in Figure 1 were calculated on the basis of the present model. To fit the experimental current vs time curves, the penetration probability p was progressively increased with an increase in the negative value of the final transmembrane potential, with a resulting increase in the steady-state value of the current. The best fit also requires a notable decrease in the overall rate constant, $k_N k_R^2$, of nucleation and growth of monazomycin channels with an increase in p. It should be noted that other sets of values of the free parameters, somewhat different from those reported in the legend of Figure 1, might fit these curves as well. In this respect, the exact values of the parameters reported here are not particularly significant. Nonetheless, the changes that must be made to these values in order to fit the changes of the sigmoidal curves with varying the transmembrane potential show a trend that does not depend on the particular choice of the set of values of the free parameters. Thus, the notable decrease in $k_N k_R^2$ with an increase in the penetration probability p (and, hence, with an increase in the number of monazomycin molecules incorporated in the BLM) is observed with all possible sets of values that provide a good fit to the experimental curves in Figure 1. This behavior can possibly be explained by considering that the high number of hydroxyl groups in a monazomycin molecule can readily form hydrogen bonds with the ether and carbonyl groups of other monazomycin molecules, within the lipid bilayer. This may cause a high rate of formation of small H-bonded clusters that may tend to grow by aggregation with other small clusters, rather than by progressive addition of single monomers. The aggregation of small clusters between themselves may have, in turn, no tendency to create pores large enough to allow the passage of ions. Thus, conductivity measurements of alamethicin single-conducting channels by the patch-clamp technique indicate that an increase in the peptide concentration causes the formation of increasingly large pores, namely, bundles formed by an increasing number of monomeric units orderly disposed around the pore.[34−37] This is possibly attributed to well-defined hydrophilic and hydrophobic faces of the alamethicin α-helices. No such well-defined structure can be envisaged in monazomycin monomers. Quite probably, the decrease in the nucleation-and-growth rate with increasing p is only apparent, since it is based on the assumption that an increase in this rate necessarily involves an increase in current. As a matter of fact, in the case of manazomycin, an increase in the nucleation rate over the growth rate, as may be expected at high monazomycin concentrations in the lipid bilayer, may cause the formation of small clusters that do not increase around a pore through the progressive uptake of further monomeric units, but aggregate between themselves, yielding larger nonconducting clusters. In this connection, it should be noted that, for a constant nucleation-and-growth rate $k_N k_R^2$, k_R may well be lower than, equal to, or higher than k_N. Therefore, the present model may account for the formation both of small dispersed clusters, when the rate constant of nucleation is higher than that of radial growth, and of larger clusters in the opposite case.

Muller et al.[5] pointed out that the monazomycin conductance changes cannot be fit by the Hodgkin and Huxley[11] scheme for the potassium channels in squid giant axon. Even though this is certainly true, the present nucleation-and-growth kinetics may satisfactorily account for the autocatalytic nature of both the current vs time curves of monazomycin and the classical Hodgkin−Huxley voltage−clamp curves of potassium channels. Thus, the same nucleation-and-growth kinetics adopted herein accounts quantitatively for the sigmoidal shape and potential dependence of the voltage−clamp curves of potassium channels in squid giant axon, using a minimum number of free parameters.[2] The formation of the voltage−clamp curves of potassium channels involves exclusively a voltage-induced, cooperative arrangement of the four subunits forming the K channel. On the other hand, the formation of monazomycin channels requires, in addition, the disaggregation of horizontal clusters, which accounts for the long foot of the current vs time curves. As distinct from potassium and melittin channels (see further), fitting of the general kinetic model of nucleation and growth to the monazomycin experimental curves requires the further assumption that the nucleation-and-growth rate leading to conducting clusters decreases notably with an increase in the population of the incorporated molecules.

Monazomycin in a tBLM. The current flowing across a tBLM, as a consequence of a potential jump inducing channel formation, behaves differently from that across a BLM. In fact, the ions moving across the lipid bilayer moiety of a tBLM are not free to diffuse in a semi-infinite aqueous medium on the trans side

(33) Muller, R. U.; Andersen, O. S. *J. Gen. Physiol.* **1982**, *80*, 427−449.

(34) Eisenberg, M.; Hall, J. E.; Mead, C. A. *J. Membr. Biol.* **1973**, *14*, 143−176.

(35) Boheim, G. *J. Membr. Biol.* **1974**, *19*, 277−303.

(36) Kolb, H.-A.; Boheim, G. *J. Membr. Biol.* **1978**, *38*, 151−191.

(37) Keller, S. L.; Bezrukov, S. M.; Gruner, S. M.; Tate, M. W.; Vodyanoy, I.; Parsegian, V. A. *Biophys. J.* **1993**, *65*, 23−27.

of the bilayer, as in the case of a BLM. Rather, they accumulate within the hydrophilic spacer moiety of the tBLM, spreading radially from the mouth of each newly formed channel, until they completely saturate it. Consequently, the current attains a maximum and then decays to zero, as soon as saturation is reached. Conversely, the charge vs time curve exhibits a sigmoidal shape, attaining a plateau that depends exclusively on the spaciousness of the hydrophilic spacer, independent of the number density of the ion channels. The model previously outlined must, therefore, be modified by associating the nucleation and growth of ion channels to the concomitant radial diffusion of the translocating ions into the hydrophilic spacer.

It should be stressed that the charge recorded at a given time t is not a direct measure of the ionic charge that has been flowing up to time t across the lipid bilayer moiety. The accumulation of this ionic charge, positive due to the negative final potential and to monazomycin being much more permeable to monovalent cations than to monovalent anions,[3] creates a potential difference across the whole metal−solution interphase, positive toward the metal. At the constant final potential following the potential jump, this potential difference must be continuously compensated for by an equal and opposite potential difference, which is produced by a flow of electrons to the electrode surface, along the external circuit. Therefore, the recorded charge $Q(t)$, once decreased by the capacitive charge recorded under otherwise identical conditions in the absence of the channel-forming molecules, is proportional, but not equal, to the ionic charge flown at time t through the channels. $Q(t)$ is calculated by assuming that the formation of each newly formed channel starts a radial diffusion of ions from its mouth. To this end, the fractional surface area covered by the ion channels formed in any given time interval (y, $y + dy$) is multiplied by the area of a circle whose radius, R_d, equals zero at time y and increases in such a way that the time derivative of its square, dR_d^2/dt, is constant. The product of these two areas is integrated over time for y varying from 0 to the observation time t, yielding a quantity that, upon correction for the overlapping of the growing diffusion circles by Avrami's approach, yields the ratio, $S_d(t)$, of the surface area covered by radial diffusion from the channel mouths to the available surface area. The charge $Q(t)$, normalized to unity, is obtained by summing the fractional surface area, $S_h\theta_0 pS$, covered by the channel mouths, to the product of S_d by the remaining fractional surface area, $(1 - S_h\theta_0 pS)$. The assumption of a constant time derivative dR_d^2/dt is justified by the expression for the concentration of a species diffusing on an infinite plane surface from a source point

$$c = \frac{M}{4\pi Dt} e^{-r^2/4Dt} \qquad (4)$$

Here, r is the distance from the source point, t is the time measured from the start of planar diffusion, D is the diffusion coefficient of the species, and M is the total amount of charge diffusing.[38] Upon disregarding the pre-exponential term with respect to the exponential one, as a first approximation, the concentration of the diffusing species maintains the same value for a constant r^2/t ratio.

The dashed curves in Figure 2 show the best fit of the calculated $Q(t)$ vs t curves to the experimental charge vs time curves for monazomycin at four different applied potentials E. A penetration probability p of unity was ascribed to the curve recorded at the more negative potential. The p values ascribed to the other three curves decrease as their potential shifts toward less-negative values, as expected. To fit the latter curves, only the product $k_N k_R^2$, which expresses the nucleation-and-growth rate of channel-forming clusters, was varied, while the remaining parameters, other than p, were left unchanged. A better fit to the two less-negative curves might have been obtained by varying further free parameters. However, such an improved fit was avoided for a more direct comparison with the voltage−clamp curves of monazomycin in BLMs (see Figure 1). It can be seen that, both in a BLM and in a tBLM, an "apparent" notable decrease in nucleation-and-growth rate with an increase in the number of incorporated molecules must be assumed, in order to account for the experimental behavior.

Melittin in a tBLM. Melittin, the principal toxic peptide of bee venom, yields sigmoidal charge vs time curves when incorporated in a tBLM, as shown in Figure 3. Evidence for an autocatalytic channel formation of melittin molecules in a BLM, as revealed by sigmoidal current vs time curves, is scarse in the literature, in spite of the fact that this peptide has been extensively investigated. Thus, the time dependence of the leakage of fluorescent dyes from vesicles brought in contact with a melittin solution has often not revealed a sigmoidal shape.[39−42] However, the time dependence of release of hemoglobin from human erythrocytes in the presence of 0.3 μM melittin exhibits a clear sigmoidal shape.[43] Conductance vs time curves of BLMs incorporating melittin from aqueous 0.5 M $NaNO_3$ were also reported to show a sigmoidal shape.[7] Similarly to monazomycin, the charge vs time curves following potential jumps from −0.200 V to different final potentials attain the same maximum limiting value, even though the penetration probability of the horizontal monomers into the lipid bilayer is expected to decrease as the final potential becomes progressively less negative. In fact, here too, the limiting value is just a measure of the ionic charge required to saturate the hydrophilic spacer. The melittin concentration of 1.4×10^{-7} M adopted in the present measurements is too low to give rise to self-association in aqueous solution.[44,45] Therefore, the calculated curves were obtained upon ignoring the initial step of disaggregation of adsorbed clusters. The dashed curves in Figure 3 were obtained by decreasing the penetration probability with a decrease in the negative value of the final potential, thus causing a decrease in the slope of the curves, but not in the height of their plateau. The best fit to the experimental curves also requires that the time derivative dR_d^2/dt be decreased with a decrease in p, and hence in the population of melittin molecules in the lipid bilayer. This can be explained by considering that the radial diffusion of ions from the mouth of newly formed channels decreases with a decrease in the flow rate of ions through them, which is measured by the M factor in eq 4. Now, a lower population is expected to give rise to ion channels composed of a lower number of monomeric units and, therefore, with smaller inner radii; this may cause a decrease in flow rate.

It is interesting to note that, if the tBLM is kept in the presence of a melittin solution for a long period of time, such as 15 min, at a potential of −0.200 V, at which melittin molecules are adsorbed flat on top of the lipid bilayer, the charge vs time curve

(38) Crank, J. *The Mathematics of Diffusion*; Oxford University Press: Oxford, 1956; p 26.

(39) Rex, S. *Biophys. Chem.* **1996**, *58*, 75−85.
(40) Hincha, D. K.; Crowe, J. H. *Biochim. Biophys. Acta* **1996**, *1284*, 162−170.
(41) Allende, D.; McIntosh, T. H. *Biochemistry* **2003**, *42*, 1101−1108.
(42) Allende, D.; Simon, S. A.; McIntosh, T. J. *Biophys. J.* **2005**, *88*, 1828−1837.
(43) Dempsey, C. E. *Biochim. Biophys. Acta* **1990**, *1031*, 143−161.
(44) Quay, S. C.; Condie, C. C. *Biochemistry* **1983**, *22*, 695−700.
(45) Schwarz, G.; Beschiaschvili, G. *Biochemistry* **1988**, *27*, 7826−7831.

following a step to a potential of −1.050 V, at which channels are formed, exhibits a long foot, as shown by curve a of Figure 5.

This behavior can only be interpreted on the basis of an initial disaggregation of horizontal clusters into horizontal monomers, as in the case of monazomycin. The corresponding dashed curve was indeed calculated upon inclusion of this initial disaggregation step. This indicates that horizontal melittin monomers adsorbed on top of the lipid bilayer tend to form clusters, as time passes. By stepping the potential back to −0.200 V and by carrying out a new potential jump to −1.050 V immediately after, the charge vs time curve recorded during the latter jump shows a very short induction period (curve b in Figure 5). The corresponding dashed curve was again calculated by ignoring the disaggregation of horizontal clusters; moreover, the best fit also requires an increase in the rate of nucleation and growth by 3 orders of magnitude with respect to the value estimated in the absence of a pretreatment at negative potentials. This strongly suggests that, during the positive potential jump, the melittin molecules are expelled from the lipid bilayer to a large extent as clusters with a hydrophobic exterior, which can be readily reincorporated following an immediately subsequent negative potential jump.

In conclusion, the sigmoidal current vs time curves exhibited by channel-forming peptides in BLMs can be satisfactorily explained by a general kinetic model of nucleation and growth of conducting clusters. Similar conclusions can be extended to change vs time curves in tBLMs. It is probable that a nucleation-and-growth mechanism is also operative when current vs time curves show the concavity constantly turned toward the time axis; in this case, this mechanism is obscured by a rate-determining penetration step of the peptide molecules into the BLM.

Acknowledgment. The authors are grateful to Prof. W. Knoll and Dr. R. Naumann (Max Planck Institute for Polymer Science, Mainz, Germany) for providing them with the DPTL thiolipid and to Prof. Joel Cohen (Laboratory of Physiology and Biophysics, University of the Pacific, S. Francisco, California) for providing them with a sample of monazomycin. Thanks are due to Ente Cassa di Risparmio di Firenze for financial support through the PROMELAB project and to MIUR (Ministry of Education, University and Research) of Italy for financial support through the grant PRIN 2004 035330.

Supporting Information Available: A general kinetic model, which accounts for the potential-independent disaggregation of adsorbed clusters into adsorbed monomers, the potential-dependent penetration of the latter into the lipid bilayer and their aggregation with channel formation by a mechanism of nucleation and growth. This material is available free of charge via the Internet at http://pubs.acs.org.

LA0636560